Primljen / Received: 19.10.2020.
Ispravljen / Corrected: 1.2.2025.
Prihvaćen / Accepted: 18.3.2025.
Dostupno online / Available online: 10.6.2025.

Investigation of the mechanical strength of cement mortars containing novel synthesised chitosan/ hydromagnesite stromatolite nano-composite

Authors:

[1]Assoc.Prof. **Selcan Karakuş**
selcan@istanbul.edu.tr

[2]Assoc.Prof. **Ayşe Elif Özsoy Özbay**
ayseelifozsoyozbay@maltepe.edu.tr
Corresponding author

[3]Assoc.Prof. **Ahmet Onur Pehlivan**
onur.pehlivan@tau.edu.tr

[2]Assist.Prof. **Ahmet Utku Yazgan**
utkuyazgan@maltepe.edu.tr

[2]Assoc.Prof. **Işıl Sanrı Karapınar**
isilkarapinar@maltepe.edu.tr

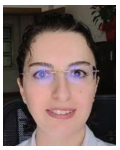

[4]Prof. **Nevin Taşaltın**
nevintasaltin@maltepe.edu.tr

[5]Prof. **Ayben Kilislioğlu**
ayben.kilislioglu@khas.edu.tr

[1] Istanbul University-Cerrahpasa, Turkey
Faculty of Engineering, Department of Chemistry
[2] Maltepe University, Turkey
Faculty of Engineering and Natural Sciences
Department of Civil Engineering
[3] Turkish-German University, Turkey
Faculty of Engineering, Department of Civil Engineering
[4] Maltepe University, Turkey
Faculty of Engineering and Natural Sciences
Department of Electrical and Electronics Engineering
[5] Kadir Has University, Turkey
Faculty of Engineering and Natural Sciences
Department of Electrical and Electronics Engineering

Research Paper

Selcan Karakuş, Ayşe Elif Özsoy Özbay, Ahmet Onur Pehlivan, Ahmet Utku Yazgan, Işıl Sanrı Karapınar, Nevin Taşaltın, Ayben Kilislioğlu

Investigation of the mechanical strength of cement mortars containing novel synthesised chitosan/hydromagnesite stromatolite nano-composite

This study introduces the use of a novel synthesised chitosan/hydromagnesite stromatolite (CHT/HS) nano-composite in cement mortars and investigates its effects on the mechanical properties. The proposed bio-based nano-composite was synthesised by a green sonication method using HS originating from Salda Lake (Burdur, Turkey). The chemical and morphological properties of HS and CHT/HS nano-composites were determined. Specimens including HS in ratios of 5 and 10 % and CHT/HS nanostructures with 0.1, 0.5, 1 and 2 % were tested for flexural and compressive strengths for 7 and 28 days. The novel synthesised CHT/HS nano-composite showed a clear enhancement in mechanical strength. These findings suggest directions for future work on different nano-filler applications.

Key words:
hydromagnesite stromatolite, cement, nano-composites, mechanical performance, microstructure

Prethodno priopćenje

Selcan Karakuş, Ayşe Elif Özsoy Özbay, Ahmet Onur Pehlivan, Ahmet Utku Yazgan, Işıl Sanrı Karapınar, Nevin Taşaltın, Ayben Kilislioğlu

Ispitivanje mehaničke čvrstoće cementnih mortova koji sadrže novi sintetizirani nanokompozit kitozan/hidromagnezit stromatolit

Ovaj rad predstavlja upotrebu novog sintetiziranog nanokompozita kitozan/hidromagnezit stromatolit (CHT/HS) u cementnim mortovima i istražuje njegove učinke na mehanička svojstva. Predloženi biološki nanokompozit sintetiziran je metodom „zelene" sonikacije primjenjujući hidromagnezit stromatolit (HS) iz jezera Salda (Burdur, Turska). Određena su kemijska i morfološka svojstva nanokompozita HS i CHT/HS. Uzorci koji sadrže HS u omjerima od 5 i 10 % i nanostrukture CHT/HS s 0,1, 0,5, 1 i 2 % ispitani su na savojnu i tlačnu čvrstoću nakon 7 i 28 dana. Novi sintetizirani nanokompozit CHT/HS pokazao je jasno povećanje mehaničke čvrstoće. Navedeni rezultati predlažu smjernice za buduci rad na različitim primjenama nanopunila.

Ključne riječi:
hidromagnezit stromatolit, cement, nanokompoziti, mehanička svojstva, mikrostruktura

1. Introduction

Recent developments in the fabrication of green nano-fillers have led to the use of nano-materials for cementitious composites in multi-disciplinary nano-technological applications. The addition of different proprortions of green nano-fillers to cement-based composites plays an important role in improving their mechanical, physical, and chemical properties. These have attracted considerable interest owing to their advantageous properties and potential eco-friendly production.

Studies have reported the high resistance and durability to chemical and physical effects and the self-healing capacity of cement using alternative green nano-materials in cementitious composites [1-3]. However, some studies have investigated whether small sizes and pores negatively affected composites because of the increased water demand in fresh concrete [4-7]. Among green materials, natural zeolite is widely used as a partial substitute for cementitious composites. The enhancement of the mechanical properties and durability of cementitious composites by substitution with zeolite has been investigated. However, the findings of earlier studies are contradictory on the effect of zeolites on cementitious composites. With the incorporation of zeolites, some studies have reported improved tensile and compressive strength of composites, whereas others have reported reduced strength. These differences in results are attributed to the particle size, purity, and dosage of natural zeolite used in the experiments [8-10]. The decrease in strength with the use of zeolite is observed especially beyond 10 % dosage of cement substitution because of the dilution effect on the cement [11-13]. Bentonite is another green filler used in cementitious composites. In one study, bentonite containing montmorillonite as the major active component was reported to increase the unconfined compressive strength of highly organic soils because of its filler effect in the case of 10 % partial replacement by cement [14]. Another study used sodium bentonite blended with metakaolin to investigate the combined effects on cement paste [5]. This combination has been reported to promote the hydration and reactivity of cement, leading to strength improvement through a better dissolution of metakaolin owing to the presence of bentonite. In a recent study, geopolymeric cement was produced using natural kaolin [15]. The study also highlighted the environmental impact of using noncalcined kaolin in the production of geopolymers and the importance of using green cement. In addition, cement pastes and mortars containing high-calcium sepiolite were tested, and the influence of substitution at varying dosages was discussed in terms of mechanical strength and rheological behaviour [16]. It was deduced that the workability of fresh specimens containing high-calcium sepiolite must be improved. The mechanical strength was also found to highest with the incorporation of 7.5 % additive. However, the drying shrinkage of the hardened specimens had to be reduced before the application of the high-calcium sepiolite in structural concrete.

In recent years, with the emergence of nano-technology, there has been a growing interest in the potential use of nano-fillers in the concrete industry owing to their distinct features that offer considerable improvements in the mechanical performance and durability of concrete. Therefore, nano-fillers with different chemical composition and morphology, and their effects on cementitious composites, have been the focus of researchers. Among these studies, the most promising results have been achieved in the incorporation of halloysite nano-tubes [17, 18], nano-metakaolin [19, 20], and nano-montmorillonite into cementitious materials [21]. A study showed that the inclusion of 0.6 % nano-montmorillonite resulted in a 13.24 % increase in compressive strength and a 49.95 % reduction in permeability of cement paste [21]. In another study, the addition of halloysite nano-clay in cement paste at a ratio of 3 % was reported to enhance the compressive strength by 24 %, with a denser microstructure [22]. This improvement was attributed to additional C-S-H formation due to the large amount of silicon dioxide on the surface of the halloysite nano-tubular structure. The results of a recent study by Morsy et al. [23] showed that with an 8 % nano-metakaolin substitution by cement, the compressive and tensile strengths of cement mortars improved by 7 % and 49 %, respectively. Nano-zeolites are another type of nano-filler used in cementitious composites.

Previous studies have focused on the use of natural materials in construction applications. However, some have explored the potential of nano-fillers in cementitious composites. Therefore, low-cost, environment-friendly, and non-toxic hydromagnesite stromatolite (HS) was preferred and a novel biomineral nano-additive was synthesised to improve the mechanical performance of cement composites.

The structure of the HS originating from Salda Lake (Burdur, Turkey) has similar chemical properties to those from the surface of Mars [24]. HS is a low-temperature hydrothermal fossil mineral in a highly alkaline (pH > 9) medium under atmospheric conditions and has a high Mg/Ca ratio [25]. However, there has been little discussion in the literature on the use of hydromagnesite in cementitious composites. In some studies, the use of hydromagnesite in a blended form with reactive MgO was investigated through various physical and chemical analyses in search of a potential magnesium (Mg)-based binder for the construction industry [26, 27]. In MgO-hydromagnesite blends, the presence of hydromagnesite improved the hydration of reactive MgO for replacement levels of 10–30 % with MgO in the paste, leading to remarkable improvements in compressive strength [26]. The proposed binder was recommended as a sustainable alternative for construction applications with further investigations of its hydration mechanisms.

Within the scope of this study, a novel chitosan/HS (CHT/HS) nano-composite was prepared using a green sonochemical method, and its mechanical and interfacial tension characteristics were investigated. The effects of the mass fraction of HS and cetyltrimethylammonium bromide (CTAB), temperature (20–50 °C) and concentration (0–0.05 ppm) on the surface properties of CHT/HS nano-composites were examined through various techniques. The scanning electron microscopy (SEM); Brunauer, Emmett,

and Teller (BET) analysis; X-ray fluorescence spectrometry (XRF), transmission electron microscopy (TEM), dynamic light scattering (DLS), and Fourier-transform infrared (FTIR) spectroscopy were used to elucidate the chemical and morphological properties of the HS and CHT/HS nano-composites.

In this study, to investigate the effects of originally introduced bio-based CHT/HS nano-composites on the mechanical properties of cement mortars, mixtures were prepared with (i) partial replacement of HS particles by 5 % and 10 % of cement and (ii) CHT/HS nano-additive inclusions with varying percentages of 0.1, 0.5, 1, and 2 %. The results show that improvements in the microstructure and mechanical performance of cementitious composites appear to support the introduction of this novel synthesised nano-additive as a potential sustainable material for construction applications.

2. Materials and methods

2.1. Materials

Ordinary Portland cement (PC 42.5 R) supplied by the Akçansa cement factory was used as the binder for the preparation of mortar samples. River sand (0–5 mm) was used as the fine aggregate. Chitosan (low molecular weight, 50,000–190,000 Da) was purchased from Sigma-Aldrich Company (Germany). Acetic acid (glacial, 100 %) was purchased from Merck Company. HS was collected from Salda Lake and washed several times with distilled water. The solution was filtered, dried at 25 °C, and passed through a 200 mesh sieve. The BET and XRF results of HS powder are listed in Table 1. The specific surface area and pore volume of HS were 20.12 m^2/g and 0.02 cm^3/g, respectively.

Table 1. Chemical composition, specific surface area, and pore volume of HS

Element	[%]
MgO	54.65
SiO_2	20.34
CaO	9.45
Al_2O_3	5.62
FeO	4.48
Fe_2O_3	2.59
TiO_2	0.06
Na_2O	2.45
MnO	0.02
MnO_2	0.05
K_2O	0.19
Cr_2O_3	0.10
Specific surface area	20.12 m^2/g
Pore volume	0.02 cm^3/g

2.2. Preparation of CHT/HS nano-composites

For cement mortars, including powder forms as the partial substitute material, the HS originating from Salda Lake was dried and ground to obtain particle sizes less than 1 mm. CHT/HS nano-composites were synthesised using the green sonication method. A solution of chitosan (0.5 g/1000 ml) in %2 (v/v) glacial acetic acid was dissolved at 25 °C. CTAB (0.5 g) and HS (0.05 g) were added to the aqueous solution, which was then homogenised for 15 min using a sonicator (35 kHz, 320 W). Then, the prepared CHT/HS nano-composites were stored at 25 °C until further use. All chemicals and reagents were analytical grade and used without further purification.

2.3. Characterisation techniques

The specific surface area and pore volume of samples were determined using the BET method using a Micromeritics ASAP 2020 (Norcross, GA, USA). An XRF spectrometer (PANalytical) was used at 40 kV and 15 A, An SEM (JEOL 63335F) was used (TedPella, double-coated, 8 mmW × 20 mL) with a 6–10 mm working distance, 0–130 Pa pressure, and voltage of 7–10 kV under a low vacuum medium. A TEM (Hitachi HighTech HT7700) was used to visualise the synthesised CHT/HS nano-composites in a high vacuum mode at 100 kV. The solution of CHT/HS nano-composites (20 µL) was dropped on a copper TEM grid and dried in a vacuum chamber for 3 h at 25 °C. An FTIR spectrometer (Perkin Elmer) was used to perform morphological characterisations of the HS and CHT/HS nano-composites (KBr powder) in the 4000–400 cm^{-1} frequency range, with a resolution of 4 cm^{-1} and eight scans. DLS (NanoPlus 3 HD zeta/nano-particle analyser) was used to analyse the particle size distribution. The drop apparatus (Fars EOR Technol., CA-ES10) was used to measure the surface tension (ST) of the liquid-liquid system under different experimental conditions, such as the mass fraction of HS (2 %, 4 %, 6 %, and 8 %), mass fraction of CTAB (1 %, 2 %, and 5 %), temperature (20–50 °C), and concentration (0–0.05 ppm). An FEI-Philips XL30 environmental scanning electron microscope equipped with an EDAX unit was used to characterise the surface morphology of the mortar specimens with secondary electron imaging at an accelerating voltage of 15 kV.

2.4. Mortar specimen preparation

All mortar mixtures were prepared with a cement: sand: water ratio of 2:2:1, considering the adequate workability of the cement paste. The specimens were cast into steel moulds with dimensions of 40 × 40 × 160 mm, with the designated mix proportions listed in Table 2. Cement mortars containing CH/HS nano-composite (configured as n-CH/HS1, n-CH/HS5, n-CH/HS10, and n-CH/HS20) were batched through the incorporation of the proposed nano-additive by 0.1, 0.5, 1, and 2 wt. % of cement in the mixture. Cement mixtures were also

Table 2. Mix proportions of mortar mixtures

Mixture	Additive [%]	Additive [g]	Cement [g]	Sand [g]	Water [g]	Superplasticiser [g]
Control	0	0	1000	1000	500	0
HS5	5	50	950	1000	500	5
HS10	10	100	900	1000	500	5
n-CHT/HS1	0.1	1	1000	1000	499	0
n-CHT/HS5	0.5	5	1000	1000	495	0
n-CHT/HS10	1	10	1000	1000	490	0
n-CHT/HS20	2	20	1000	1000	480	0

prepared with partial replacement of HS particles with 5 % and 10 % of cement, denoted as HS5 and HS10, respectively. In the preliminary stage of this study, HS5 and HS10 specimens without superplasticiser addition were found to have very low workability, resulting in compaction problems when casting into moulds. Therefore, a superplasticiser was used the HS5 and HS10 specimens to level the flowability values of these mixtures to the control mixture.

Cement mixtures were prepared using a Hobart mixer. For the cement composites containing HS particles, cement, sand, and HS were dry mixed for 1 min, followed by the addition of water and mixing for 2 min. For specimens with nano-composites, a nano-additive in liquid form was added to the mixing water to obtain a uniform distribution before mixing with dry ingredients. All specimens were demolded after 24 h and cured in water tanks at a temperature of 20 °C.

2.5. Flowability of mortar specimens

The flowability of mortar mixtures was tested in compliance with ASTM C1437-15 [28]. A flow mould (50 mm height) was filled with the mixture in two layers on a jumping table, with each layer tamped 20 times. The mould was then lifted and 25 strokes were applied to the mixture for 15 s using the flow table. The average diameter of the spread fresh mixture measured along two perpendicular directions was obtained to evaluate the flow of mortar mixtures.

2.6. Mechanical tests

Mechanical tests were performed on prismatic specimens with dimensions of 40 × 40 × 160 mm as specified in TS EN 196-1 [29] to evaluate the 7- and 28-day flexural and compressive strengths of mortar mixtures. For each sample configuration, six specimens were tested using a three-point loading procedure with an MTS closed-loop servo-hydraulic test system. Displacement-controlled flexural loading was applied to the specimens at a rate of 0.5 mm/min. Vertical displacement data were obtained to moderate the loading rate in a closed-loop system using a linear variable differential transformer placed under the midspan of prismatic specimens. The variations in strain mechanisms due to the inclusion of additives in mortar mixtures were monitored using a displacement-controlled loading ramp during the testing procedure. From the three-point loading test results, the flexural stress values were obtained by the following equation:

$$\sigma = \frac{3PL}{2bd^2} \quad (1)$$

where σ is the flexural stress, P is the maximum flexural load; and d, b, and L are the height, width, and span length of the prismatic specimen, respectively. Half prisms of cracked specimens after flexural testing were utilised for the compression test, which was performed according to TS EN 196-1 [29]. Force-controlled compressive loading was applied at a speed of 0.6 MPa/s, while the testing data were recorded at 10 Hz with a data acquisition system.

3. Results and discussion

3.1. Characterisation of HS and CHT/HS nano-composites

In this study, HS originating from Salda Lake were used for the first time as a biomineral additive in cement composites. There have been several studies on the enhanced mechanical properties of cement composites and the improvement of the interfaces of the cement structure; however, few studies have been reported on the mechanical properties of biomineral-based cement composites [30-32].

According to the literature, the homogeneous distribution of composites significantly affected their mechanical properties. Therefore, to examine the distribution of HS and CHT/HS nano-composites, morphological analyses were conducted using SEM, TEM, and DLS, as shown in Figures 1 and 2. The SEM micrograph images confirmed that the surface morphology of HS was an irregular and heterogeneous structure (Figure 1). The SEM results showed that the morphology of nano-particles was a nano-sized spherical structure in the range of 330–375 nm. In our previous study [33], the surface area of HS was found to be 20.12 m^2/g. The BET results showed that the surface area of the CHT/HS nano-composite was 109.20 m^2/g. When the results were compared with the surface area of pure HS, it was found that the CHT/HS nano-composite had large surface areas.

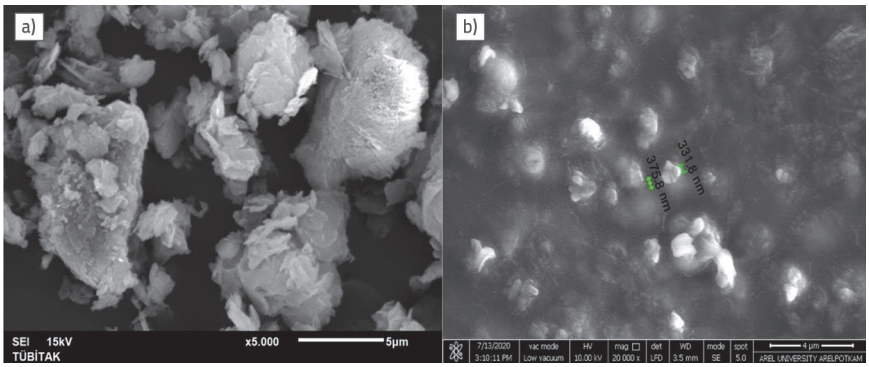

Figure 1. SEM micrographs of: a) HS with x5.000 magnification; b) CHT/HS nano-composite with x20.000 magnification

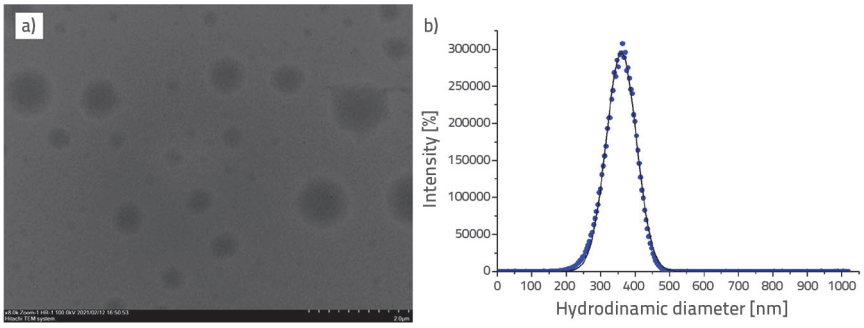

Figure 2. a) TEM micrograph; b) DLS curve of CHT/HS nano-composite

The TEM technique was used to characterise the surface of the synthesised CHT/HS nano-composites, as shown in Figure 2. According to the TEM results, the CHT/HS nano-composites had a spherical shape with sizes ranging from 200 to 400 nm (Figure 2.a). In addition, the nano-composites were well-separated in the structure. A polymeric shell was observed in the TEM images. The size of the CHT/HS nano-composite was determined using the DLS technique, as shown in Figure 2.b. The hydrodynamic diameter and polydispersity index values of CHT/HS nano-composites were measured as 360.25 ± 5.70 nm and 0.175, respectively. These results confirmed that aggregation did not occur in the medium for the CHT/HS nano-composite. The morphological results were compatible with the obtained SEM and DLS results. It was concluded that the polymer matrix acted as a stabilising and capping agent [34] for the fabrication of green CHT/HS nano-composites. To the best of our knowledge, this is the first study on the green fabrication of synthesised HS-based nano-composites for cement applications.

The FTIR technique was used to investigate functional groups of structure in the region between 4000 and 400 cm^{-1} for HS and CHT/HS nano-composites. The results of the FTIR analysis of the HS and CHT/HS nano-composites are shown in Figure 3. According to these results, absorption bands of HS were observed at 1480 cm^{-1} (CH_3 bending), 1420 cm^{-1} (C-H asymmetric bending vibration), 1000 cm^{-1} (Si-O-Si stretching vibration), and 885 cm^{-1} (Si-O-Si stretching vibration) [33]. Absorption bands of CHT/HS nano-composites were observed at 3240 cm^{-1} (-NH_2 and O–H vibrations), 2875 cm^{-1} (NH stretching), 1480 cm^{-1} (CH_3 bending), 1599 cm^{-1} (amide I), and 1022 cm^{-1} (skeletal vibration of C-O stretching). Comparison of FTIR results of HS and CHT/HS nano-composites showed a slight decrease in the intensity of absorption bands owing to the possible interaction of functional groups on the surface of the nano-structure [35]. Differences in the characteristic spectral bands occurred when HS and CHT were mixed owing to electrochemical interactions. Owing to the FTIR results, compared with the HS, a considerable shift in the position of bands toward the lower wavenumber region is visible in the FTIR spectra of CHT/HS nano-composites (3523 cm^{-1} to 3240 cm^{-1}, 1000 cm^{-1} to 1018 cm^{-1}). In addition, it was observed that the characteristic band between 3500 cm^{-1} and 3000 cm^{-1}, corresponding to the OH stretching vibration, increased in comparison with pure HS due to a new interaction by the hydrogen bond [36, 37] formed between the HS and CHT matrix owing to the physical and chemical changes in the nano-structure.

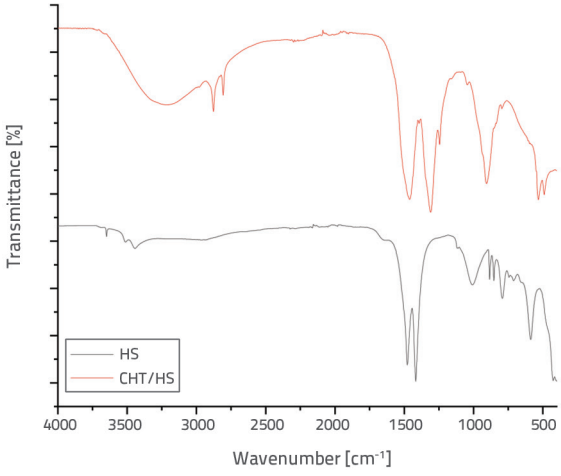

Figure 3. FTIR analysis of HS and CHT/HS nano-composites

3.2. Surface tension measurement of CHT/HS nano-composites

There are few studies on the ST of nano-systems in the literature. The main focus of this study was on the effect of the ST of CHT/HS nano-composites/water on the mass fraction (%) of HS, mass fraction (%) of CTAB, and temperature of the nano-system. The effect of the mass fraction (%) of HS on the ST is shown in Figure 4. The ST of nano-structure/water from 40.35 mN/m

to 14.55 mN/m by changing nano-composite concentrations from 0 to 0.05 ppm (pressure: 1 atm, temperature: 25 °C) was measured. The experimental results showed that the ST of the nano-structure/water increased with the increase in the CHT/HS nano-composite concentration [38].

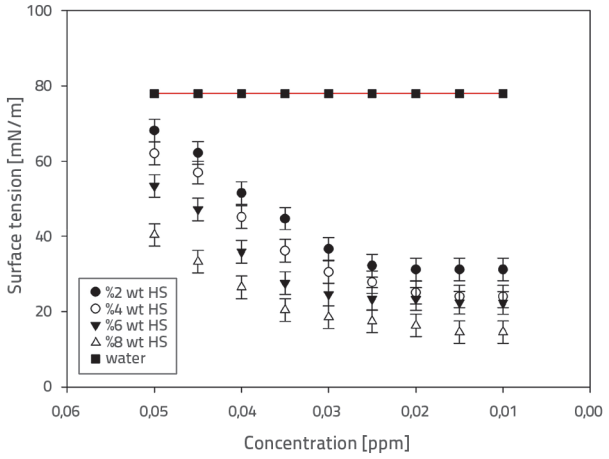

Figure 4. The effect of the mass fraction (%) of HS in CHT/HS nano-composites on the surface tension of the nano-composite/water system

The effect of temperature (20 to 50 °C) on the ST of CHT/HS (%8) nano-composites/water system is shown in Figure 5. According to the experimental data, when the temperature was increased, the ST decreased as the attraction forces between particles decreased [38].

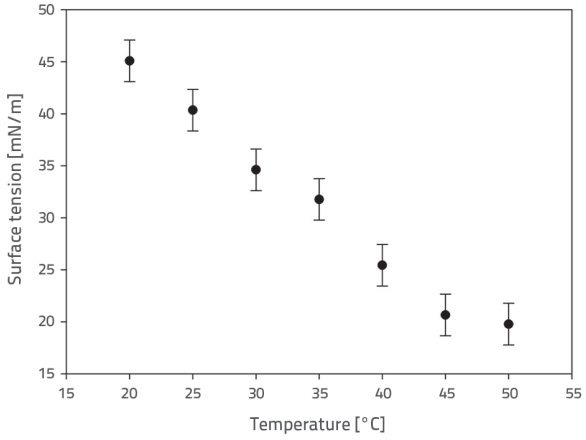

Figure 5. The effect of the temperature (20–50 °C) on the surface tension of CHT/HS (%8) nano-composites/water system

The interfacial tension decreased when HS was added to the aqueous solution (Figure 6). Therefore, it was assumed that the addition of the CTAB (5 %) improved the stability of the nano-system and affected the surface properties of the CHT/HS nano-composite. It was hypothesised that weak interactions with liquid molecules occurred because of the low solubility of HS.

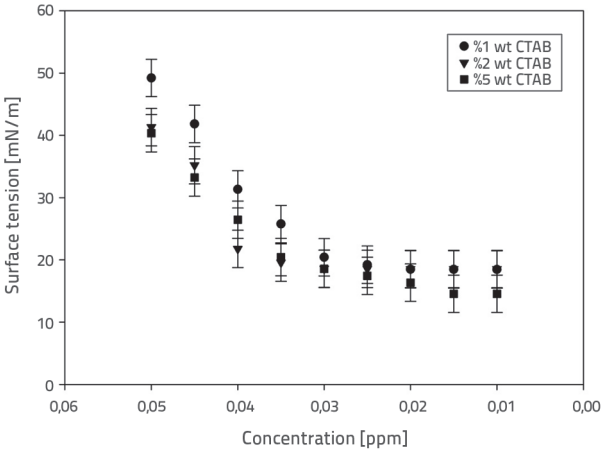

Figure 6. The effect of the mass fraction (%) of CTAB on the surface tension of the nano-composite/water system

3.3. Flowability of mortar mixtures

The flowability of mortar mixtures was measured, and the results are presented in terms of the ratio of the mortar spread diameter to the mould base diameter in percentages in Figure 7.

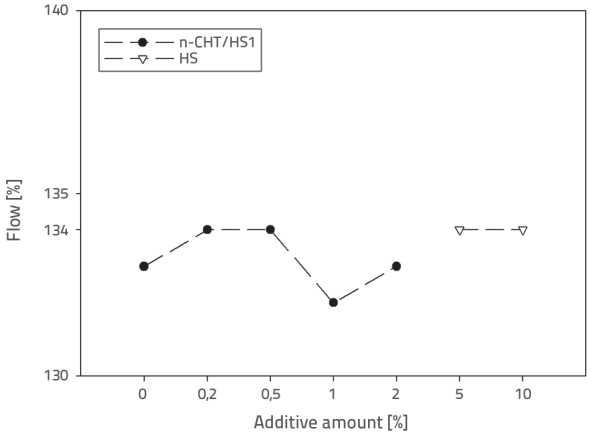

Figure 7. Flowability results

Table 3. Flowability and unit weight results of the specimens

Mixture	Additive [%]	Fresh density [kg/m³]	Bulk air-dry density [kg/m³]	Flowability [%]
Control	0	2233	2158	133
HS5	5	2182	2085	134
HS10	10	2115	2011	134
n-CHT/HS1	0.1	2227	2150	132
n-CHT/HS5	0.5	2284	2211	133
n-CHT/HS10	1	2311	2240	134
n-CHT/HS20	2	2310	2234	134

With the superplasticiser effect, the flowability of the HS-containing mortars reached the flowability level of the control specimen as presented in Table 3. On the other hand, for the nano-mixtures, although there has not been much difference in flowability results, considering that no superplasticiser was used, a small increase in flowability was observed with increasing nano-particle dosages. In fact, in previous studies showed that owing to the high surface area of nano-fillers and high water absorption, the decrease in the flowability of mortars, including nano-particles, was predicted [22, 39]. Therefore, the slight increase in the flowability of the n-CHT/HS mixtures might be attributed to the effect of the bio-based polymer used in this study.

3.4. Testing of mechanical strength

For all batches of mortar mixtures, the inclusion of the CH/HS nano-mixture had a significant effect on strength development, while the results from both compressive and flexural testing tended to decrease with the increase in additive content for specimens prepared with HS in powder form. This may be related to the particle size and low reactivity of HS particles used in their natural form without the application of any additional process. Thus, this low reactive HS has not been involved much in hydration reactions and may have only acted as a microfiller material, eventually creating a lighter and relatively good matrix structure. On the other hand, the reactivity of such materials was enhanced by increasing the specific surface area and decreasing the mean grain size. In this study, nano-sized particles were synthesised by incorporating HS particles, thus increasing the overall reactivity of these Mg-based products. To overcome the agglomeration effect reported in the literature, these nano-particles were utilised with a polymer matrix. The agglomeration problem was addressed in both the flowability and mechanical tests. Moreover, the nano-structured forms of HS with CHT exhibited adequate performance, modifying the mechanical performance of the cementitious composites.

The compressive and flexural strength test results for the 7- and 28-day specimens are shown in Figs. 8 and 9, respectively. Considering the overall mechanical strength results, the addition of nano-mixtures below 1 % was ineffective in inducing alterations in both flexural and compressive strengths. Regarding the 7- and 28-day results of the HS specimens, the compressive and flexural strengths were found to be lower than those of the control specimens, indicating that the incorporation of HS in powder form did not lead to improvements in the mechanical performance of cement composites. Based on the 28-day results, for the mixtures containing n-CH/HS, the highest compressive strength was achieved for a 2 % dosage, with a 7.5 % increase compared with the control specimen. However, the optimum dosage for the flexural strength was found to be 1 %, with a 4 % increase for mortars containing n-CHT/HS. This limited increase in flexural strength with respect to compressive strength may be due to the limited formation of nucleation sites in the interfacial transition zones, which are known to significantly affect the flexural performance. However, rather than nucleation sites in the interfacial transition zone, the filler effect of the nano-particles most likely contributed to the relatively higher increase in the compressive strength [40, 41]. When 7-day compressive strength results were investigated, it is seen that for specimens with n-CHT/HS, higher additive percentages (1 % and 2 %) affected the strength adversely, contrary to the 28-day results. This finding may be explained by the latter hydration reaction due to the inclusion of the additive. Similar findings were observed in the flexural strength results.

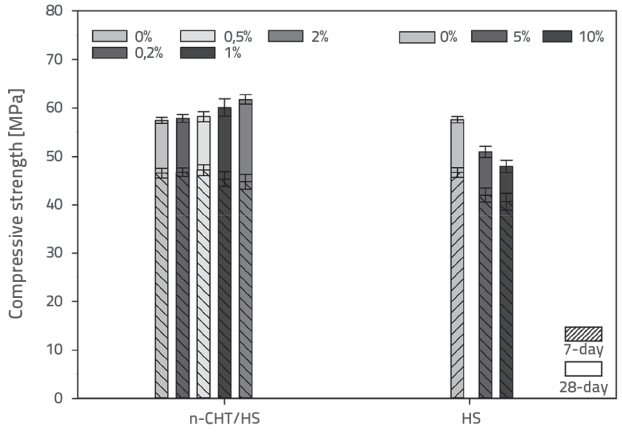

Figure 8. 7- and 28-day compressive strength results

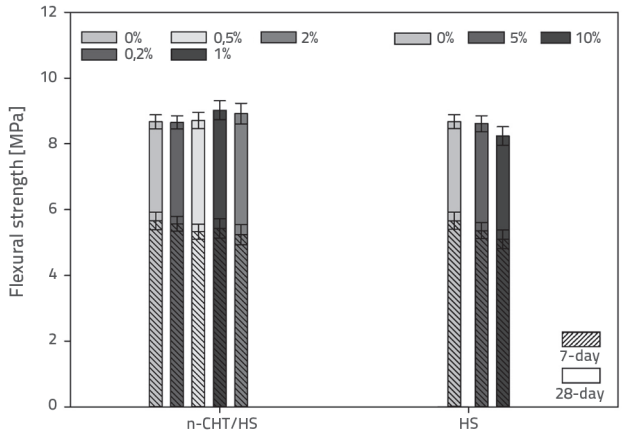

Figure 9. 7- and 28-day flexural strength results

3.5. Microstructural investigation

Microstructural investigations were conducted on fragmented pieces from specimens after 7 and 28 days of curing. An SEM image of the specimens incorporating HS10 in powder form is shown in Figure 10. Microscopic investigations showed that the powder HS specimens were well-dispersed in the cementitious mortar, creating a considerably good and homogenous internal structure which might be linked to adequate results despite mortar formation with a lower weight. This homogenous structure can be explained by the effective integration of particles with Mg content into the cement hydration mechanism, which

may also be inferred from the low deviations of the mechanical test results.

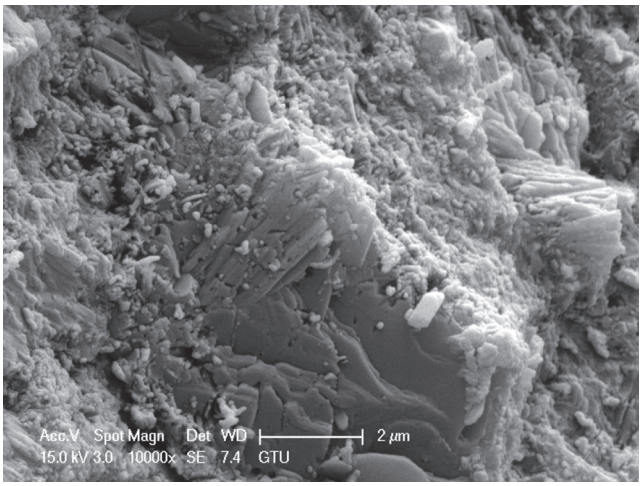

Figure 10. SEM micrograph of specimens incorporating HS10 in powder form: multi-layered Ca(OH)$_2$ formations

Specimens with n-CHT/HS additives were found to have better mechanical results. Microstructural imaging confirmed these findings, with a better internal structure configuration increasing with the amount of nano-additive.

In Figure 11, n-CHT/HS20 specimens with 2 % nano-additive inclusion were visualised with a different C-S-H formation, with a considerable amount of Mg content approved by the comparison electron diffraction spectroscopy (EDS) analyses presented in Figs. 12 and 13 for the control and n-CHT/HS20 specimens, respectively. Comparing the EDS results, the Mg K peak was clearly observed for the n-CHT/HS20 specimen, whereas such a finding was not observed for the control specimen. The nano-scale configuration of hydromagnesite particles may have participated as enhanced nucleation sites [42], and with the high reactivity supplied by the high specific surface area and good dispersion of the synthesised polymer matrix, may have induced a pozzolanic reaction to create denser hydration products incorporating Mg and some $MgOH_2$ (brucite) [43]. In the presence of Mg, the formation of larger nuclei and higher lateral growth was also detected in another study [44].

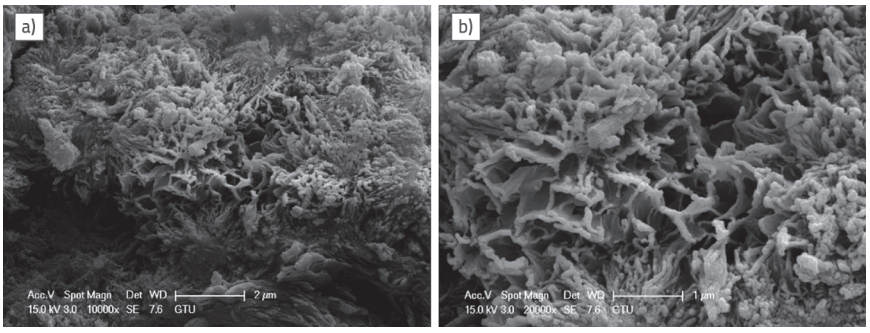

Figure 11. C-S-H formations with Mg content for n-CHT/HS20 specimens at (a) 10000x and (b) 20000x magnifications

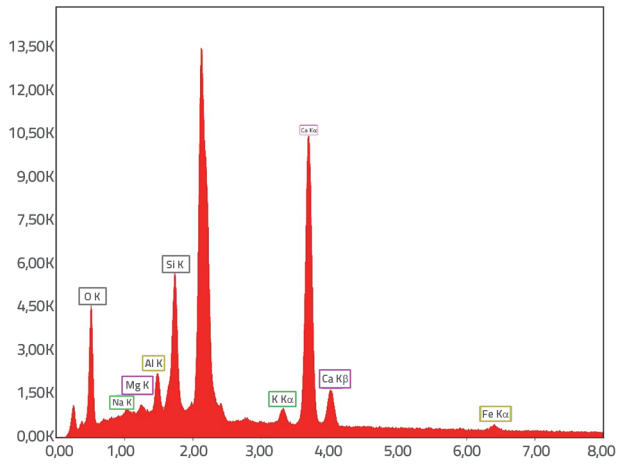

Figure 12. EDS analysis of control specimen

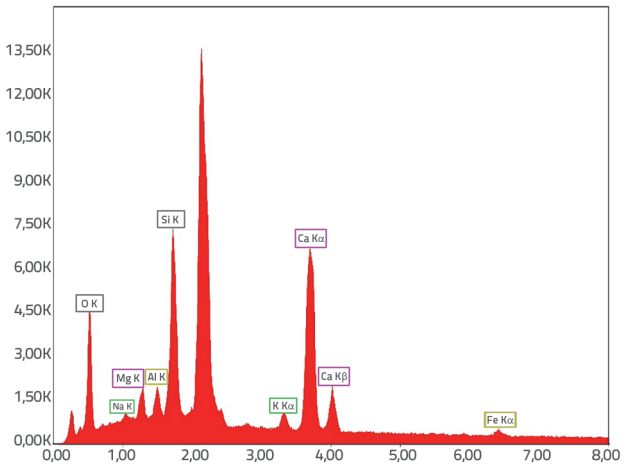

Figure 13. EDS analysis of n-CHT/HS20 specimen

4. Conclusion

A novel CHT/HS nano-composite was prepared and incorporated into cement mortars to examine the effects of the nano-structure on mechanical properties. CHT/HS nano-composites were synthesised from CHT and HS using a green sonochemical technique. CHT/HS nano-composites were characterised using SEM, TEM, DLS, XRF, BET, and FTIR to determine their chemical and morphological properties. STs of CHT/HS nano-composites were experimentally determined as a function of the mass fraction (%) of HS, mass fraction (%) of CTAB, and temperature. The experimental results showed that the ST of CHT/HS nano-composites/water changed with the mass fraction (%) of HS, mass fraction (%) of CTAB, and temperature of the nano-system.

Under the determined optimum conditions, the average particle size for the CHT/HS nano-composite was ~350 nm, with a homogeneous particle distribution and surface area of 109.201 m^2/g.

With regard to the effects of the novel nano-structure on mechanical behaviour, cement mortar specimens containing HS in ratios of 5 and 10 %, and CHT/HS nano-structures with varying contents of 0.1, 0.5, 1, and 2 %, were tested for flexural and compressive strengths for 7 and 28 days. The results show that the use of HS in powder form did not have a clear contribution to the strength except for the advantage of producing lightweight specimens. A distinct observation that emerged from the data comparison was the strength improvement of the specimens including n-CHT/HS additives. The results revealed that the optimum usage of n-CHT/HS for the highest compressive strength was 2 % with a 7.5 % increase, and 1 % with a 4 % increase in flexural strength. This enhancement in the mechanical strength of n-CHT/HS mixtures may be attributed to the good dispersion induced by the synthesised polymer matrix and the filler effect of nano-particles that densify the microstructure of the mixtures.

This study is a preliminary attempt to present the preparation and the first time a hydromagnesite nano-structure was used to evaluate the effects of the proposed novel morphologies on the mechanical properties of cement mortars. The results so far have been very encouraging for improving the mechanical properties and microstructure of cement mortars using the originally synthesised CHT/HS. In conclusion, this research will give rise to further investigations on the use of nano-sized additives in cementitious composites.

REFERENCES

[1] Du, X., Hou, D., Liang, C., Li, C., Sun, Z., Zheng, S.: Heating induced hierarchically mesoporous adsorbent derived from natural hydromagnesite for highly efficient defluoridation of water, J. Taiwan Inst. Chem. Eng., 111 (2020), pp. 119–129, https://doi.org/10.1016/j.jtice.2020.04.015

[2] Razavi, S.M., Nazarpour, H., Hosseinali Beygi, M.: Investigation of the efficacy of nano-silica on mechanical properties of Green-Engineered Cementitious Composite (GECC) containing high volume natural zeolite, Construction and Building Materials, 291 (2021), Paper 123246, https://doi.org/10.1016/J.CONBUILDMAT.2021.123246

[3] Wang, D., Dong, S., Ashour, A., Wang, X., Qiu, L., Han, B.: Biomass-derived nanocellulose-modified cementitious composites: A review, Materials Today Sustainability, 18 (2022), Paper 100115, https://doi.org/10.1016/J.MTSUST.2022.100115

[4] Memon, S.A., Arsalan, R., Khan, S., Lo, T.Y.: Utilization of Pakistani bentonite as partial replacement of cement in concrete, Construction and Building Materials, 30 (2012), pp. 237–242, https://doi.org/10.1016/j.conbuildmat.2011.11.021

[5] Wei, J., Gencturk, B.: Hydration of ternary Portland cement blends containing metakaolin and sodium bentonite, Cement and Concrete Research, 123 (2019), Paper 105772, https://doi.org/10.1016/j.cemconres.2019.05.017

[6] Dabić, P., Barbir, D.: Implementation of natural and artificial materials in Portland cement, Hemijska Industrija, 74 (2020), pp. 147–161, https://doi.org/10.2298/HEMIND191216014D

[7] Luhar, S., Luhar, I., Shaikh, F.: Nano-modified green cementitious composites, Recent Advances in Nano-Tailored Multi-Functional Cementitious Composites, (2022), pp. 305–346, https://doi.org/10.1016/B978-0-323-85229-6.00003-2

[8] Azad, A., Saeedian, A., Mousavi, S.F., Karami, H., Farzin, S., Singh, V.P.: Effect of zeolite and pumice powders on the environmental and physical characteristics of green concrete filters, Construction and Building Materials, 240 (2020), Paper 117931, https://doi.org/10.1016/j.conbuildmat.2019.117931

[9] Ahmadi, B., Shekarchi, M.: Use of natural zeolite as a supplementary cementitious material, Cement and Concrete Composites, 32 (2010), pp. 134–141, https://doi.org/10.1016/j.cemconcomp.2009.10.006

[10] Burris, L.E., Juenger, M.C.G.: Effect of calcination on the reactivity of natural clinoptilolite zeolites used as supplementary cementitious materials, Construction and Building Materials, 258 (2020), Paper 119988, https://doi.org/10.1016/j.conbuildmat.2020.11998

[11] Najimi, M., Sobhani, J., Ahmadi, B., Shekarchi, M.: An experimental study on durability properties of concrete containing zeolite as a highly reactive natural pozzolan, Construction and Building Materials, 35 (2012), pp. 1023–1033, https://doi.org/10.1016/j.conbuildmat.2012.04.038

[12] Vejmelková, E., Koňáková, D., Kulovaná, T., Keppert, M., Žumár, J., Rovnaníková, P., Keršner, Z., Sedlmajer, M., Černý, R.: Engineering properties of concrete containing natural zeolite as supplementary cementitious material: Strength, toughness, durability, and hygrothermal performance, Cement and Concrete Composites, 55 (2015), pp. 259–267, https://doi.org/10.1016/j.cemconcomp.2014.09.013

[13] Xu, W., Chen, J.J., Wei, J., Zhang, B., Yuan, X., Xu, P., Yu, Q., Ren, J.: Evaluation of inherent factors on flowability, cohesiveness and strength of cementitious mortar in presence of zeolite powder, Construction and Building Materials, 214 (2019), pp. 61–73, https://doi.org/10.1016/j.conbuildmat.2019.04.115

[14] Wong, L.S., Hashim, R., Ali, F.: Utilization of sodium bentonite to maximize the filler and pozzolanic effects of stabilized peat, Engineering Geology, 152 (2013), pp. 56–66, https://doi.org/10.1016/j.enggeo.2012.10.019

[15] Pelisser, F., Bernardin, A.M., Michel, M.D., da Luz, C.A.: Compressive strength, modulus of elasticity and hardness of geopolymeric cement synthetized from non-calcined natural kaolin, Journal of Cleaner Production, 280 (2021), https://doi.org/10.1016/j.jclepro.2020.124293

[16] Wu, C., Kou, S.: Effects of high-calcium sepiolite on the rheological behaviour and mechanical strength of cement pastes and mortars, Construction and Building Materials, 196 (2019), pp.105–114, https://doi.org/10.1016/j.conbuildmat.2018.11.130

[17] Haw, T.T., Hart, F., Rashidi, A., Pasbakhsh, P.: Sustainable cementitious composites reinforced with metakaolin and halloysite nanotubes for construction and building applications, Applied Clay Science, 188 (2020), Paper 105533, https://doi.org/10.1016/j.clay.2020.105533

[18] Allalou, S., Kheribet, R., Benmounah, A.: Effects of calcined halloysite nano-clay on the mechanical properties and microstructure of low-clinker cement mortar, Case Studies in Construction Materials, 10 (2019), Paper e00213, https://doi.org/10.1016/j.cscm.2018.e00213

[19] Morsy, M.S., Alsayed, S.H., Aqel, M.: Hybrid effect of carbon nanotube and nano-clay on physico-mechanical properties of cement mortar, Construction and Building Materials, 25 (2011), pp. 145–149, https://doi.org/10.1016/j.conbuildmat.2010.06.046

[20] El-Gamal, S.M.A., Amin, M.S., Ramadan, M.: Hydration characteristics and compressive strength of hardened cement pastes containing nano-metakaolin, HBRC Journal, 13 (2017), pp.144–121, https://doi.org/10.1016/j.hbrcj.2014.11.008

[21] Chang, T.P., Shih, J.Y., Yang, K.M., Hsiao, T.C.: Material properties of portland cement paste with nano-montmorillonite, Journal of Materials Science, 42 (2007), pp. 7478–7487, https://doi.org/10.1007/s10853-006-1462-0

[22] Farzadnia, N., Abang Ali, A.A., Demirboga, R., Anwar, M.P.: Effect of halloysite nanoclay on mechanical properties, thermal behavior and microstructure of cement mortars, Cement and Concrete Research, 48 (2013), pp. 97–104, https://doi.org/10.1016/j.cemconres.2013.03.005

[23] Morsy, M.S., Alsayed, S.H., Aqel, M.: Effect of Nano-clay on mechanical properties and microstructure of ordinary Portland cement mortar, International Journal of Civil & Environmental Engineering, 10 (2010), pp. 23–27

[24] Edwards, H.G.M., Moody, C.D., Newton, E.M., Villar, S.E.J., Russell, M.J.: Raman spectroscopic analysis of cyanobacterial colonization of hydromagnesite, a putative martian extremophile, Icarus, 175 (2005), pp. 372–381, https://doi.org/10.1016/j.icarus.2004.12.006

[25] Braithwaite, C.J.R., Zedef, V.: Living hydromagnesite stromatolites from Turkey, Sedimentary Geology, 92 (1994), pp. 1–5, https://doi.org/10.1016/0037-0738(94)90051-5

[26] Kuenzel, C., Zhang, F., Ferrándiz-Mas, V., Cheeseman, C.R., Gartner, E.M.: The mechanism of hydration of MgO-hydromagnesite blends, Cement and Concrete Research, 103 (2018), pp. 123–129, https://doi.org/10.1016/j.cemconres.2017.10.003

[27] Winnefeld, F., Epifania, E., Montagnaro, F., Gartner, E.M.: Further studies of the hydration of MgO-hydromagnesite blends, Cement and Concrete Research, 126 (2019), Paper 105912, https://doi.org/10.1016/j.cemconres.2019.105912

[28] ASTM international: C1437 - Standard test method for flow of hydraulic cement mortar, 2013.

[29] TSI: TS EN 196-1 - Methods of Testing cement - Part 1: Determination of Strength, Ankara, Turkey, 2016.

[30] Mangadlao, J.D., Cao, P., Advincula, R.C.: Smart cements and cement additives for oil and gas operations, 2015.

[31] Li, Z., Wang, H., He, S., Lu, Y., Wang, M.: Investigations on the preparation and mechanical properties of the nano-alumina reinforced cement composite, Materials Letters, 60 (2006), pp. 356–359, https://doi.org/10.1016/j.matlet.2005.08.061

[32] Benazzouk, A., Douzane, O., Mezreb, K., Quéneudec, M.: Physico-mechanical properties of aerated cement composites containing shredded rubber waste, Cement and Concrete Composites, 28 (2006), pp. 650–657, https://doi.org/10.1016/j.cemconcomp.2006.05.006

[33] Karakuş, S., Taşaltın, N., Taşaltın, C., Kilislioğlu, A.: Comparative study on ultrasonic assisted adsorption of Basic Blue 3, Basic Yellow 28 and Acid Red 336 dyes onto hydromagnesite stromatolite: kinetic, isotherm and error analysis, Surfaces and Interfaces, 20 (2020), Paper 100528, https://doi.org/10.1016/j.surfin.2020.100528

[34] Li, F., He, T., Wu, S., Peng, Z., Qiu, P., Tang, X.: Visual and colorimetric detection of uric acid in human serum and urine using chitosan stabilized gold nanoparticles, Microchemical Journal, 164 (2021), Paper105987, https://doi.org/10.1016/j.microc.2021.105987

[35] Marrakchi, F., Hameed, B.H., Hummadi, E.H.: Mesoporous biohybrid epichlorohydrin crosslinked chitosan/carbon–clay adsorbent for effective cationic and anionic dyes adsorption, International Journal of Biological Macromolecules, 163 (2020), pp. 1079–1086, https://doi.org/10.1016/j.ijbiomac.2020.07.032

[36] Fatoni, A., Hariani, P.L., Hermansyah, Lesbani, A.: Synthesis and characterization of chitosan linked by methylene bridge and schiff base of 4,4-diaminodiphenyl ether-vanillin, Indonesian Journal of Chemistry, 18 (2018), pp. 92–101, https://doi.org/10.22146/ijc.25866

[37] Wang, Y., Cen, C., Chen, J., Fu, L.: MgO/carboxymethyl chitosan nanocomposite improves thermal stability, waterproof and antibacterial performance for food packaging, Carbohydrate Polymers, 236 (2020), Paper 116078, https://doi.org/10.1016/j.carbpol.2020.116078

[38] Huminic, A., Huminic, G., Fleaca, C., Dumitrache, F., Morjan, I.: Thermal conductivity, viscosity and surface tension of nanofluids based on FeC nanoparticles, Powder Technology, 284 (2015), pPaper 78–84, https://doi.org/10.1016/j.powtec.2015.06.040

[39] Rao, G.A.: Investigations on the performance of silica fume-incorporated cement pastes and mortars, Cement and Concrete Research, 33 (2003), pp. 1765–1770, https://doi.org/10.1016/S0008-8846(03)00171-6

[40] Siang Ng, D., Paul, S.C., Anggraini, V., Kong, S.Y., Qureshi, T.S., Rodriguez, C.R., Liu, Q. feng, Šavija, B.: Influence of SiO2, TiO2 and Fe2O3 nanoparticles on the properties of fly ash blended cement mortars, Construction and Building Materials, 258 (2020), Paper 119627, https://doi.org/10.1016/j.conbuildmat.2020.119627

[41] Wang, L., Zheng, D., Zhang, S., Cui, H., Li, D.: Effect of nano-SiO2 on the hydration and microstructure of Portland cement, Nanomaterials, 6 (2016), https://doi.org/10.3390/nano6120241

[42] Lothenbach, B., Scrivener, K., Hooton, R.D.: Supplementary cementitious materials, Cement and Concrete Research, 41 (2018), pp. 1244–1256, https://doi.org/10.1016/j.cemconres.2010.12.001

[43] Stephan, D., Dikoundou, S.N., Raudaschl-Sieber, G.: Hydration characteristics and hydration products of tricalcium silicate doped with a combination of MgO, Al2O3 and Fe2O3, Thermochimica Acta, 472 (2008), pp. 64–73, https://doi.org/10.1016/j.tca.2008.03.013

[44] Bazzoni, A., Suhua, M., Wang, Q., Shen, X., Cantoni, M., Scrivener, K.L.: The effect of magnesium and zinc ions on the hydration kinetics of C3S, Journal of the American Ceramic Society, 97 (2014), pp. 3684–3693, https://doi.org/10.1111/jace.13156